MWCNT-PVA composite as Q-switched initiator in passive erbium doped fiber laser

M. M. MAFROOS[1], A. HAMZAH[2,*], K. M. MUSTHAFA[3]
[1]*Division of Electrical, Electronics and Telecommunication Engineering Technology, Institute of Technology University of Moratuwa, Sri Lanka*
[2]*Malaysia-Japan International Institute of Technology, Universiti Teknologi Malaysia, Jalan Sultan Yahya Petra, Kuala Lumpur, Malaysia.*
[3]*School of Engineering and Emerging Technologies, Barzan University College, Bin Derham Plaza, Doha, Qatar*

Saturable absorbers (SA) synthesized with varying ratios of multi-walled carbon nanotube (MWCNT) and polyvinyl alcohol (PVA) host were used in a laser cavity experiment to investigate a passively Q-switched erbium-doped fiber laser (EDFL) for its pulsed-laser specifications. Using solution-casting process, MWCNT-PVA SA films were fabricated in two distinct ratios: 1:1 and 2:3. MWCNT-PVA SAs were exhibiting 1557.98 nm and 1557.48 nm for pulsed laser respectively, and 1560.72 nm for continuous wavelength at 56 mW input pump power. Using an identical EDFL fibre laser cavity, the pulse energy, output power, repetition rate, pulse width, and signal to noise ratio (SNR) characteristics were compared. The briefest pulse width obtained using 1:1 and 2:3 MWCNT-PVA SAs was 4.43 μs, whereas the maximum repetition rates of 89.13 kHz and 134.2 kHz yielded 3.94 μs, the narrowest pulse. In a passively Q-switched EDFL laser, the 2:3 MWCNT-PVA SA demonstrated the maximum output power of 2.84 mW, while the 1:1 MWCNT-PVA SAs displayed the highest pulse energy of 24.57 nJ with an SNR value of 42 dB.

(Received December 3, 2024; accepted December 4, 2025)

Keywords: Q-switching, MWCNT, Electro-optic, Gain medium, EDFL, Saturable absorber

1. Introduction

The Q-switched fiber laser is a type of high-performance laser, which operates primarily based on the laser's Q-factor [1]. Because of its high peak power, Q-switched lasers find extensive application in material processing, telecommunication, tattoo removal, range finding (Lidar) [2], optical sensors, medicine [3], and data storage systems. A high intensity pulsed laser can be built either actively or passively with the Q-switched fiber laser, which is an easy-to-use, compact, flexible, and economical method [4]. While the passive Q-switching strategy does not call for any additional bulging electronic devices, the active Q-switching method requires an additional device, either an electro-optic or an acousto-optic device [5]. However, fabricating SAs that are compact and affordable is necessary.

Numerous research studies have explored the development of Q-switched fiber lasers using a variety of techniques. These include employing different gain media such as 1-micron Ytterbium-doped fibre [6], 1.5-micron Erbium-doped fibre [7], 2.0-micron Thulium-doped fibre [8], and 2.1-micron Holmium-doped fibre [9]. Researchers have also investigated connecting various pumped lasers including solid-state [10], semiconductor, and gas lasers. Additionally, different fabrication methods such as mechanical exfoliation [11], electrochemical exfoliation [12], solution-casting [13] and drop-casting [14] have also been utilized. The use of different host materials like polymethyl methacrylate (PMMA) [15], polyamide, polyvinyl alcohol (PVA) [16], and polycarbonate (PC) have also been explored. Furthermore, studies have implemented different types of cavities such as linear cavities and ring cavities to enhance laser performance and versatility in various applications [17].

Various types of SAs have been integrated into numerous configurations of Q-switched fiber laser cavities. These SAs fall into two main categories: real and synthetic [18]. Synthetic SAs such as the nonlinear optical loop mirror (NOLM) and nonlinear polarization rotation (NPR) require consistent maintenance within the laser cavity [19]. However, achieving high-energy pulses efficiently often necessitates the use of real SAs, which directly modulate intra-cavity losses [20]. Examples of real SAs include graphene, PbS quantum dots (QDs), carbon nanotubes (CNTs), topological insulators (TIs), transition metal dichalcogenides (TMDs), transition metal oxides (TMOs), and black phosphorus (BP) [21]. Among these options, carbon-based SAs are particularly favored due to their exceptional performance characteristics. These include straightforward fabrication, cost-effectiveness, easy-integration, zero-bandgap, ultrafast recovery, wide bandwidth, high damage threshold, extensive absorption across various wavelengths, and exceptional electrical and optical properties [22].

MWCNTs stand out among other carbon-based SAs due to their superior mechanical strength, enhanced thermal stability, and ability to absorb more photons per nanotube owing to their higher mass density from multiple walls [23]. These thermal properties are particularly advantageous for developing high-power ultrafast lasers. The unique

structure of MWCNT, consisting of densely stacked graphene sheets, contributes to these favorable characteristics. Each MWCNT has a maximum nanostructure diameter of 15 nm. In this study, passively Q-switched Erbium-doped fiber laser (EDFL) employing MWCNT and PVA was selected as the host polymer due to its proven attributes including excellent film-forming capabilities [24], exceptional flexibility [25], water solubility, transparency, non-toxicity, and high durability [20]. The material may be able to withstand this heat for a while if it has sufficient heat dissipation. However, frequent high-intensity exposure can cause interface deterioration (weakening of CNT-PVA binding), polymer degradation, and nanotube damage. Reduced modulation depth, increased insertion loss, and unstable Q-switching performance are some signs of MWCNT-PVA SA degradation.

Numerous articles about MWCNT SA were published. However, there has never been a comparison of two distinct ratios between MWCNT and PVA published. MWCNT-PVA SAs in two different ratios (1:1 and 2:3) were fabricated to achieve high-energy pulses in this experiment. The MWCNT-PVA SAs were individually sandwiched in a fiber ferrule connector within the ring cavity without altering the experimental design. Various output laser parameters such as pulse train (mV), output power (mW), pulse energy (nJ), signal-to-noise ratio (dB), pulse width (μs), and repetition rate (kHz) were compared across each SA configuration.

2. Methodology

In this study, MWCNT-PVA SAs were fabricated using the solution-casting method [3] to fabricate the SAs with ratios of 1:1 and 2:3. A standardized experimental setup, illustrated in Fig. 1, was employed to meticulously compare the output parameters of both ratios of MWCNT-PVA SAs, aiming to pinpoint the optimal ratio for maximizing the performance of the MWCNT-PVA SAs.

2.1. Experiment setup: Q-switched EDFL ring cavity configuration

Fig. 1 illustrates the schematic configuration of the passively Q-switched EDFL laser cavity. The cavity consists of a 980/1550 nm wavelength division multiplexer (WDM), which is connected to the 980 nm LD (Q-photonics, QFLD-405-20S) as a unidirectional power source in the benchtop laser controller (GOOCH & HOUSEGO, EM595). It is linked to the 980 nm port of the WDM, which separates the wavelength-dependent laser into 980 nm and 1550 nm ports. Together with a gain medium of a 1.7-m EDF with numerical aperture (NA) range of 0.23 – 0.26, an isolator is introduced to ensure no backward reflection is generated.

A 95/5 output coupler is connected in the cavity, where 95% of laser is fed back into the cavity, while the remaining 5% is characterized as the laser output. The core and cladding diameters of the EDF is 6.3 μm and 125 μm, respectively. The fabricated SAs were sandwiched within a fiber ferrule using an FC/PC connector. The laser cavity was pumped with a 980 nm laser diode via WDM. The spectra of the EDFL with and without SAs were inspected using the optical spectrum analyzer (OSA; Yokogawa, AQ6370D). Due to a change in Refractive Index and SA Nonlinear Properties, 1:1 and 2:3. MWCNT-PVA SAs are exhibiting different wavelength of 1557.98 nm and 1557.48 nm for pulsed laser respectively, and 1560.72 nm for continuous wavelength (without SA) at 56 mW input pump power The output pulse was inspected using a mixed domain oscilloscope (MDO; TEKTRONIX, MDO3024). The coupled signal was then connected to an oscilloscope in order to analyze the pulse repetition rate (F_r) and pulse width (Δ_t), which are the temporal parameters of the generated pulse train. Fr can also be calculated for linear and ring cavities from Eq. (1) and Eq. (2)[26],

$$F_r = \frac{c}{2Ln} \text{ (Linear Cavity)} \quad (1)$$

$$F_r = \frac{c}{Ln} \text{(Ring Cavity)} \quad (2)$$

where F_r is the repetition rate, c is the speed of light (m/s), n is the refractive index, and L is the cavity length (m).

The average optical output power, P_{avg} is measured with an optical power meter (OPM; THORLABS, PM100D), while the pulse energy, U is calculated from Eq. (3) [27].

$$U = \frac{P_{avg}}{F_r} \quad (3)$$

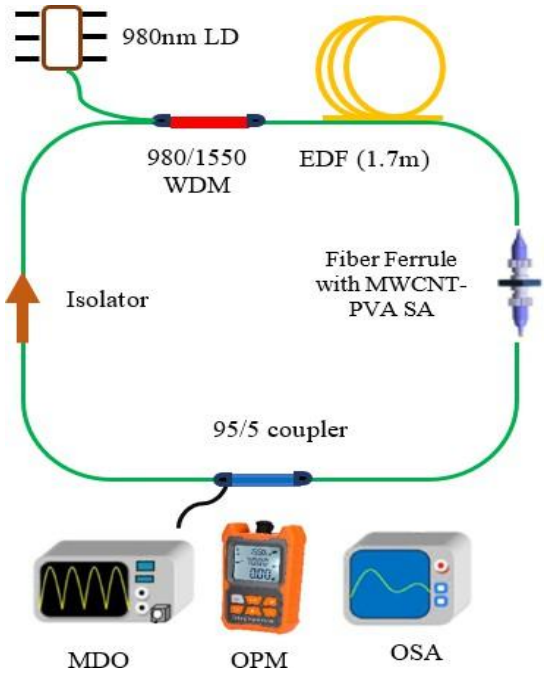

Fig. 1. Experiment setup of the passively Q-switched EDFA (colour online)

2.2. Fabrication of MWCNT-PVA saturable absorber

Fig. 2 depicts the fabrication of MWCNT-PVA SAs. Initially, 2.5 mg of sodium dodecyl sulphate (SDS) measured by electronic balance (OHAUS, AX324) was mixed with 250 ml of deionized (DI) water using a hot-plate stirrer (DATHAN SCIENTIFIC, MSH-20D) at a stirring speed of 360 rpm and temperature of 200 °C for an hour to obtain the SDS solution. SDS is essential for dispersing MWCNTs in water, ensuring uniformity during fabrication of saturable absorbers. Then, 45 ml of deionized-sodium dodecyl sulphate (DI–SDS) mixer solution was mixed with 4.5 mg of MWCNT powder and stirred for 24 hours and this mixture then underwent an ultrasonication bath with a sonicator (FISHERBRAND, FB1505) [25]. Afterwards, 1 g of PVA powder was mixed with 120 ml DI water and stirred thoroughly using the hot-plate stirrer for another 24 hours.

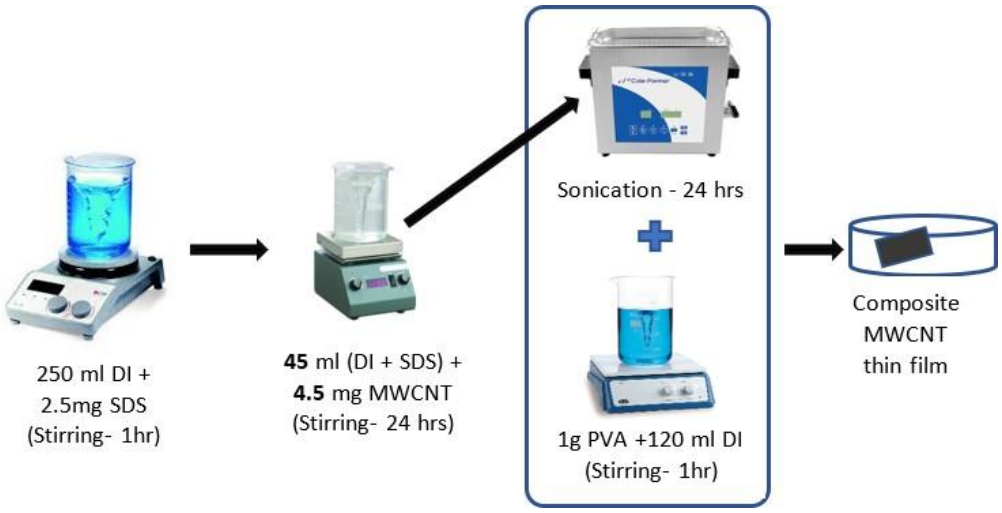

Fig. 2. Fabrication of thin film MWCNT SA (colour online)

The PVA solution was then mixed with MWCNT mixer solutions in two different ratios (1:1 and 2:3) as mentioned in Table 1 and sonicated for 72 hours. The final solution was poured into a petri dish and left to dry for two days [7].

MWCNT: PVA (ratio)	MWCNT: PVA (ml)
1:1	2.5 ml: 2.5 ml
2:3	2.0 ml: 3.0 ml

Table 1. Ratio between MWCNT solution and PVA solution

The MWCNT-PVA thin film SA was afterwards peeled from the petri dish as shown in Fig. 3.

(a) *(b)*

Fig. 3. Fabrication of MWCNT: PVA solution (a) 1:1 and (b) 2:3 (colour online)

Once the two SAs were fabricated, a small portion of the thin SA film of around 1 mm × 1 mm was incorporated alternately in the cavity to form the SA in the 50-cm diameter ring cavity as shown in Fig. 4. The MWCNT-

PVA SA was sandwiched within the fiber ferrule using a matching gel index.

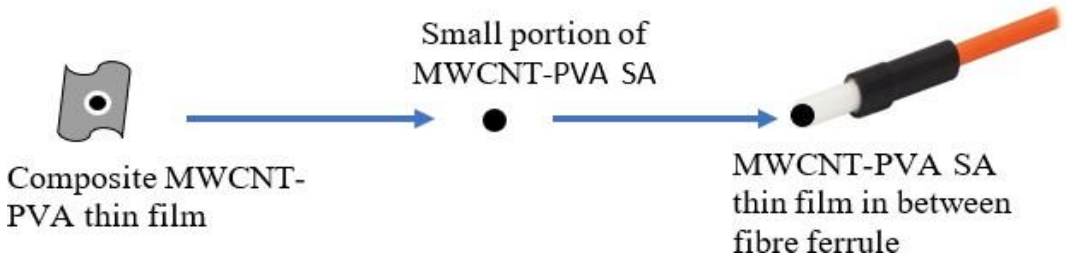

Fig. 4. Sandwiching MWCNT-PVA SA in between fiber ferrule (colour online)

2.3. Characterization of MWCNT-PVA SA

Spectroscopic characterization is one of the most important processes in progressing the Q-switched fiber laser experiment. Spectrophotometric characterization has two subcategories: optical characterization and physical characterization. In order to characterize SA optically, surface morphology was studied using field emission scanning electron microscopy (FESEM) and Raman characterization [28]. A physical characterization is performed to observe the 3D image whereby the thickness of the SA was determined using a 3D measuring laser microscope. Before being inserted into the laser cavity, the MWCNT-PVA SA needed to be characterized.

2.3.1. Raman characterizion

In this experiment, WiTec Alpha 300R Raman spectroscopy was used to ascertain the Raman characterization. The SA material was deposited onto a microscope slide to observe the Raman scattering with respect to Raman characterization as shown in Fig. 5.

Fig. 5. WiTec Alpha 300R Raman spectroscopy (colour online)

This was used to study the disorder of arrangement in sp^2 carbon structure in carbon-based SAs. Higher frequency G (graphite area), D (defect region), and 2D or G- (second-order Raman scattering from D-band variation) modes can be seen from the corresponding Raman spectra.

The G and 2D modes indicate that the used MWCNT-PVAs are multilayered graphene flakes [8]. The MWCNT-PVA SA exhibits signature peak at around D (1349 cm^{-1}), G (1574 cm^{-1}) and 2D (2687 cm^{-1}) as shown in Fig. 6.

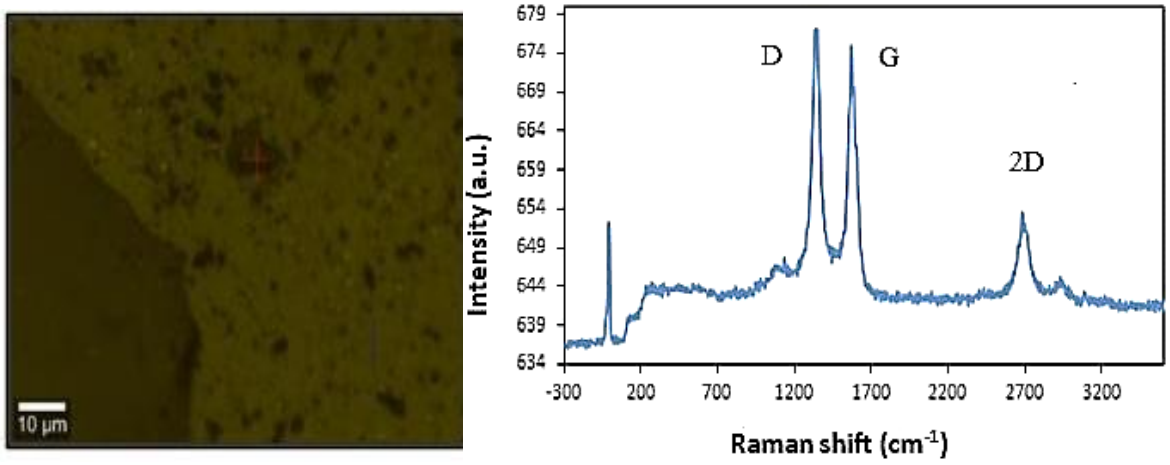

Fig. 6. Raman spectroscopy image and Raman spectrum of MWCNT-PVA SA (colour online)

2.3.2. FESEM characterization - surface morphology

JSM-7800F FESEM microscopy was used to characterize the surface morphology of MWCNT-PVA SA films as prescribed following the FESEM characterization technique. This would provide a variety of information about material surfaces. The FESEM is an essential tool for collecting large area electron backscatter diffraction (EBSD) maps at low magnifications without distortion as well as analyzing the fine structural morphology of nanomaterials at 1,000,000X magnification with sub-1nm resolution. It was simple to determine whether an SA material is evenly distributed throughout the PVA matrix from the FESEM image. Instead of using light, FESEM spectroscopy works with electrons.

Very low electron energies reveal extremely fine surface patterns. In this study, SAs are characterized by FESEM using JSM-7800F microscopy. The surface morphology of MWCNT-PVA SA is depicted in Fig. 7 for both the 1:1 and 2:3 ratios.

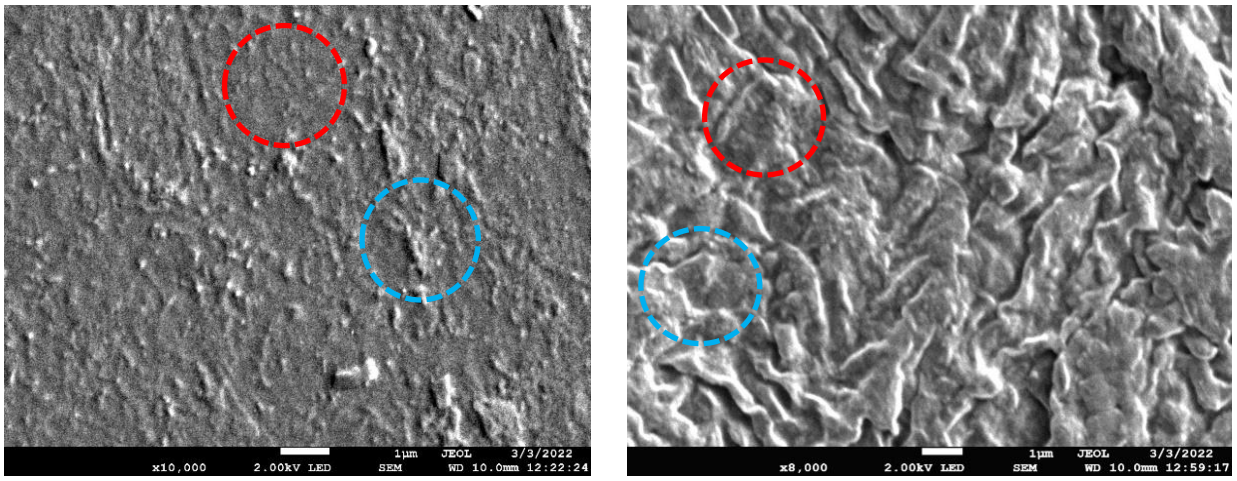

(a) *(b)*

Fig. 7. Surface morphology of (a) MWCNT-PVA (1:1) and (b) MWCNT-PVA (2:3) SA (colour online)

2.3.3. Physical characterization – thickness measurement

The purpose of physical characterization is to capture quick depth composition images and clear 3D images. The Olympus LEXT OLS4100 3D measuring laser microscope provides the physical characterization of the SA material. The camera captured many images from different focus positions.

This provides observation angles from the x, y and z axes in the electronic monitor display. Overall, the SA images could clearly be observed using a digital microscope. The thickness measurements of MWCNT-PVA ratio of 1:1 and 2:3 are shown in Fig. 8 (a) and (b). The thickness of MWCNT-PVA SA thin films of ratios 1:1 and 2:3 was measured to be 32.5 µm and 11.7 µm, respectively. Since additional nanotubes offer more absorption centers that can be bleached at high intensities, increasing the concentration of MWCNT usually results in a rise in the modulation depth. A higher MWCNT concentration generally lowers the saturation intensity, as more absorbing centers make it easier to reach the saturation threshold.

It is evident that the thickness of MWCNT–PVA SA

thin films is closely related to the ratio and volume of the MWCNT solution used during fabrication. Notably, both the ratio and volume of the MWCNT solution exhibit a direct relationship with the average thickness of the resulting thin films. This observed correlation supports the accuracy and consistency of the MWCNT solution's ratio and volume in the thin film fabrication process.

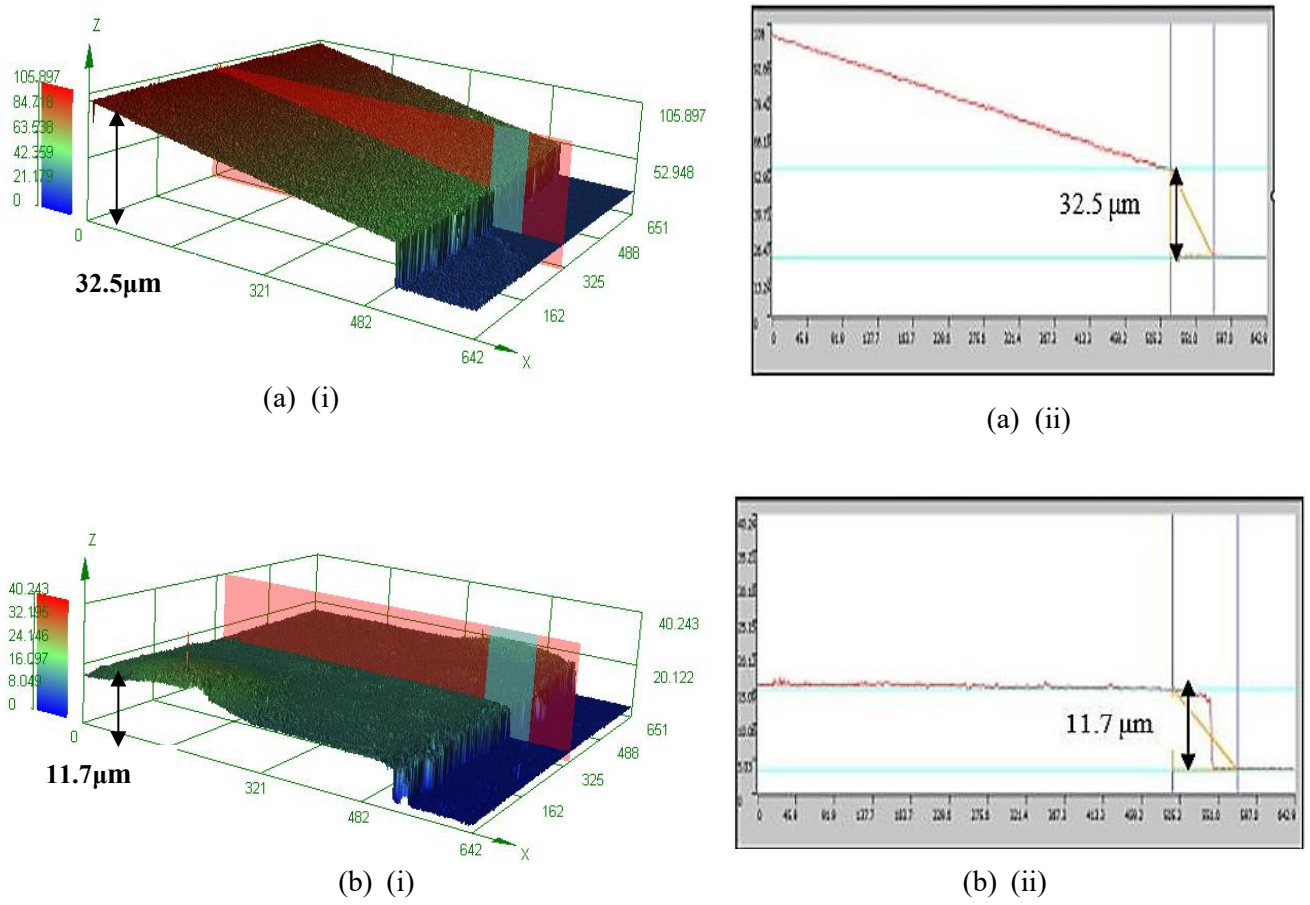

Fig. 8. (a) (i) 3D image and (ii) Thickness profile of 1:1 MWCNT-PVA thin film; (b) (i) 3D image and (ii) Thickness profile of 2:3 MWCNT-PVA thin film (colour online)

3. Results and discussion

The output parameters were compared after individual 1:1 and 2:3 MWCNT-PVA SAs were inserted into the laser cavity. To achieve a stable pulse in the cavity, the input pump was progressively increased for each SA. In the ring cavity, a continuous wave lasing was observed at 54 mA of pump power. Using a 980 nm pump laser for the two different ratios, the output spectra of the EDFL are displayed in Fig. 9 both with and without the MWCNT-PVA SA. After inserting the 1:1 MWCNT-PVA SA into the cavity, Fig. 9(a) demonstrates that the Q-switched laser began to oscillate at a wavelength of 1557.98 nm. After inserting the 2:3 MWCNT-PVA SA into the cavity, Fig. 9(b) demonstrates that the Q-switched laser began to operate at a wavelength of 1557.48 nm.

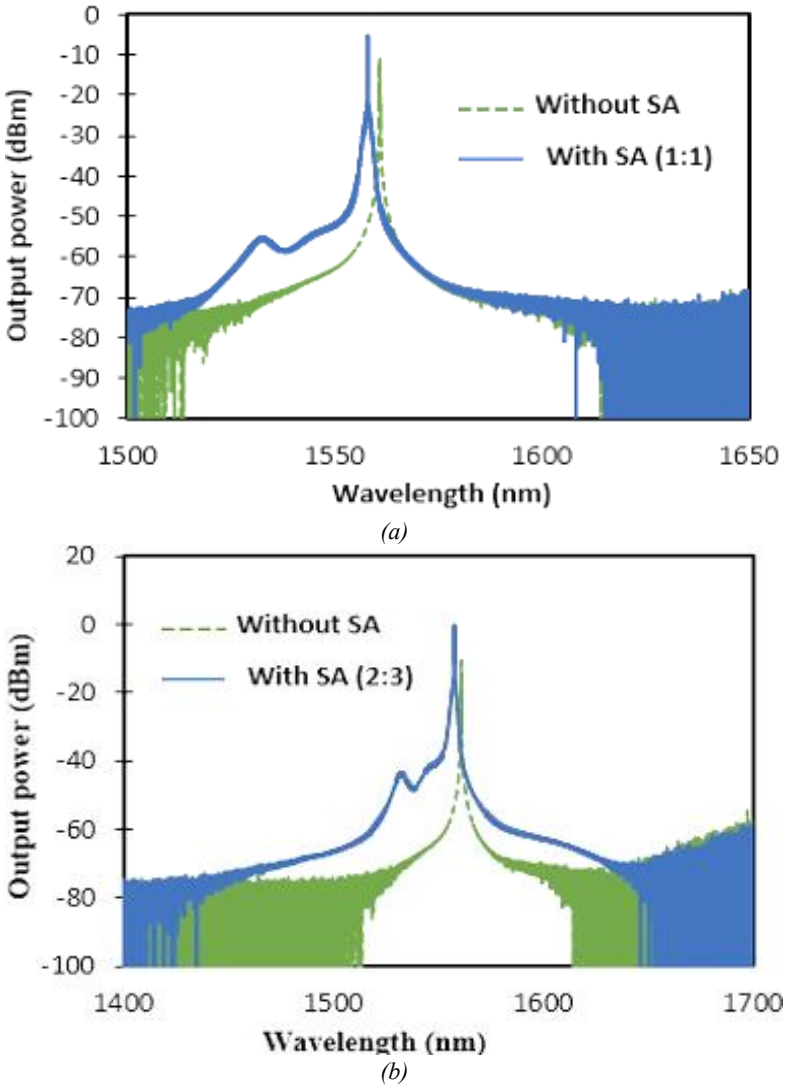

Fig. 9. Output spectra of the EDFL with and without MWCNT-PVA SA (a) 1:1 (b) 2:3 (colour online)

2.4. Comparing output values by varying the ratio of MWCNT-PVA SA

Using an oscilloscope, stable pulse patterns were examined for each ratio of 1:1 and 2:3 MWCNT-PVA SAs by adjusting the input pump. When the input pump of the 1:1 and 2:3 MWCNT-PVA passively Q-switched EDFL was varied, a stable pulse train was established; the ranges are 31.3 – 121.5 mW and 83.6 – 177.6 mW, respectively.

The repetition rate and pulse width values were recorded while the steady pulse was being observed from oscilloscope.

The Q-switched operations trace of MWCNT-PVA SAs with a concentration ratio of 1:1, recorded at a maximum pump power of 177.6 mW, is shown in Fig. 10. With a repetition rate of 89.13 kHz and a pulse width of 4.43 μs, the 1:1 MWCNT-PVA SA has a pulse period of 11.22 μs.

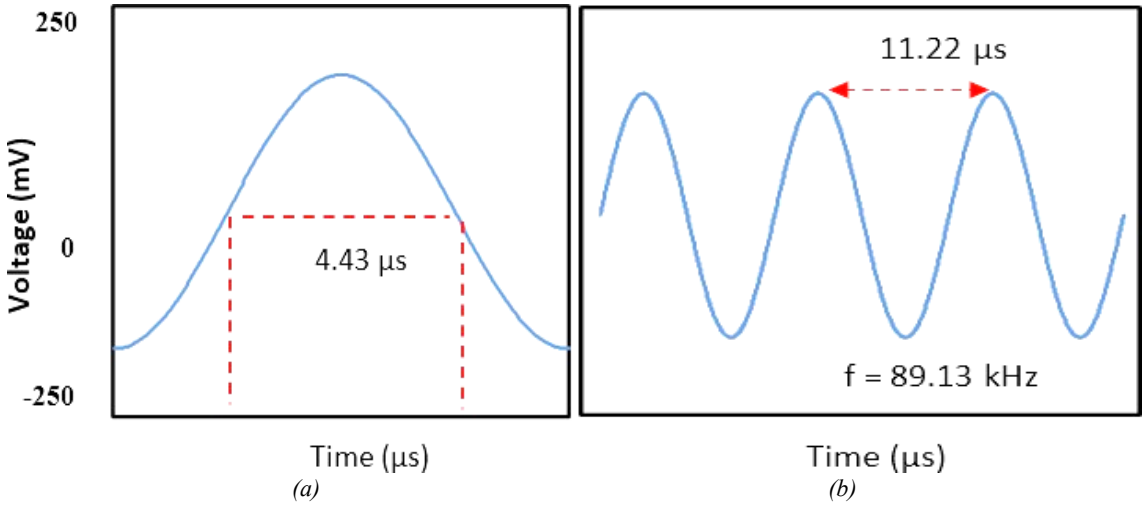

(a) *(b)*

Fig. 10. Oscilloscope trace of (a) pulse width and (b) pulse period of MWCNT-PVA (1:1) SA (colour online)

Fig. 11 depicts the oscilloscope trace of Q-switched operation for MWCNT-PVA SA with a concentration ratio of 2:3 which was recorded at maximum pump power of 177.6 mW. The pulse period for 2:3 MWCNT-PVA SA was 7.45 µs, resulting in a repetition rate of 134.2 kHz and a pulse width of 3.94 µs.

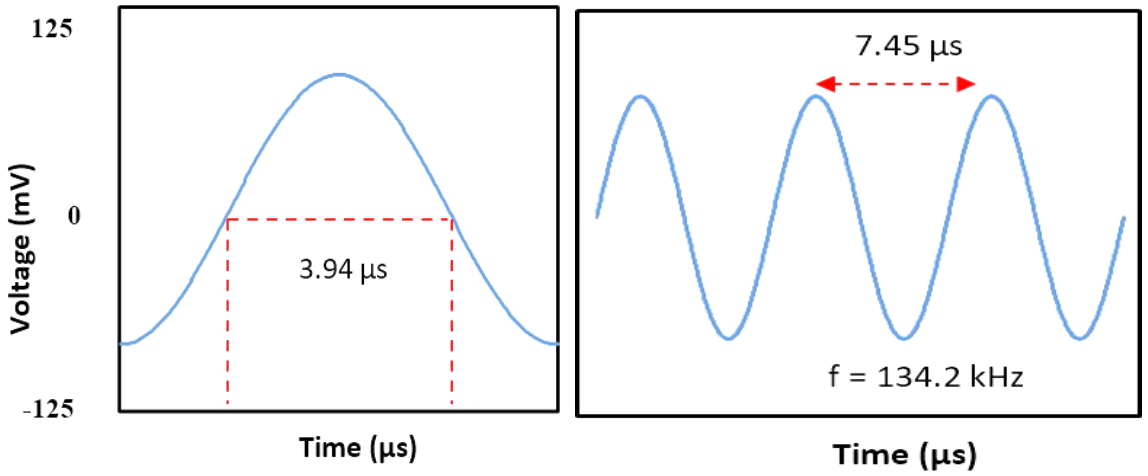

(a) *(b)*

Fig. 11. Oscilloscope trace of (a) pulse width and (b) pulse period of MWCNT-PVA (2:3) SA

Fig. 12(a) shows the comparison of repetition rates while Fig. 12(b) shows the comparison of pulse widths of the Q-switched EDFL when placing the 1:1 and 2:3 MWCNT-PVA SAs. In terms of repetition rate, 2:3 MWCNT-PVA Q-switched fiber laser reached the highest repetition of 134.2 kHz and lowest pulse width of 3.94 µs at the pump power of 95 mW. MWCNT-PVA Q-switched EDFL reached the repetition rate of 89.13kHz and pulse width of 4.43 µs at its highest pump power of 121.5 mW, whereas graphene Q-switched EDFL reached the repetition rate of 115 kHz and pulse width of 3.9 µs at its highest pump power of 127.1 mW. Because of their intrinsic saturable absorption properties and ultrafast recovery time, MWCNT-PVAs have shown promise for Q-switched fiber lasers.

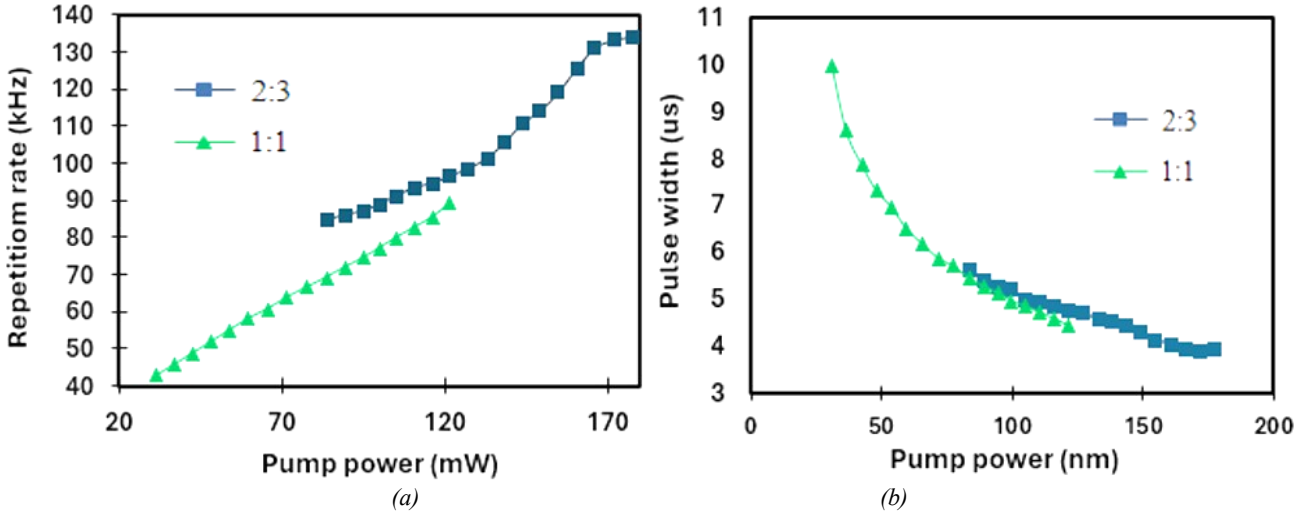

(a) *(b)*

Fig. 12. (a) Repetition rate and (b) Pulse width of MWCNT- PVA (1:1) and (2:3) (colour online)

The input pump power was gradually increased until a stable pulse train was obtained in the cavity. Fig. 13 (a) shows the comparison of output power for the two different ratios of 1:1 and 2:3 MWCNT-PVA while varying the input pump power. The maximum output power for 1:1 MWCNT-PVA EDFL is 2.19 mW, whereas 2.84 mW for 2:3 MWCNT-PVA Q-switched EDFL. When comparing the output pulse energy for the two different ratios of SAs in the same Q-switched EDFL, 1:1 MWCNT- PVA Q-switched EDFL obtained the highest pulse energy of 24.57 nJ at pump power of 121.5mW, whereas 2:3 MWCNT-PVA Q-switched EDFL attained 21.15 nJ at pump power of 177.6 mW as shown in Fig. 13(b). Higher modulation depth and lower satuaration intensity in 1:1 MWCNT: PVA SA provide the higher pulse energy.

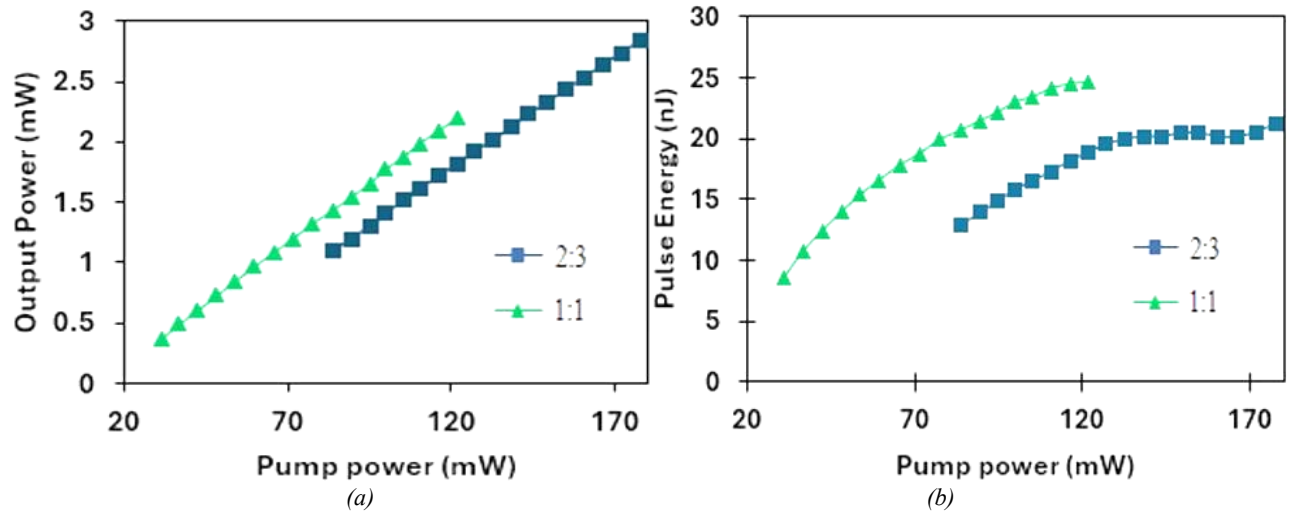

(a) *(b)*

Fig. 13. (a) Output power (b) Pulse energy of MWCNT-PVA (1:1) and (2:3) (colour online)

Fig. 14(a) indicates the signal to noise ratio (SNR) value of 1:1 MWCNT-PVA SA. The maximum value of 42 dB was achieved when placing MWCNT-PVA SA in the laser cavity. Fig. 14(b) indicates the signal to noise ratio (SNR) value of 2:3 MWCNT-PVA SA. The maximum value of 41 dB was achieved when placing the 2:3 MWCNT-PVA SA in the laser cavity. This change occurs due to the change in refractive index variation, gain medium efficiency, miss alignment losses, micro bending and macro bending losses.

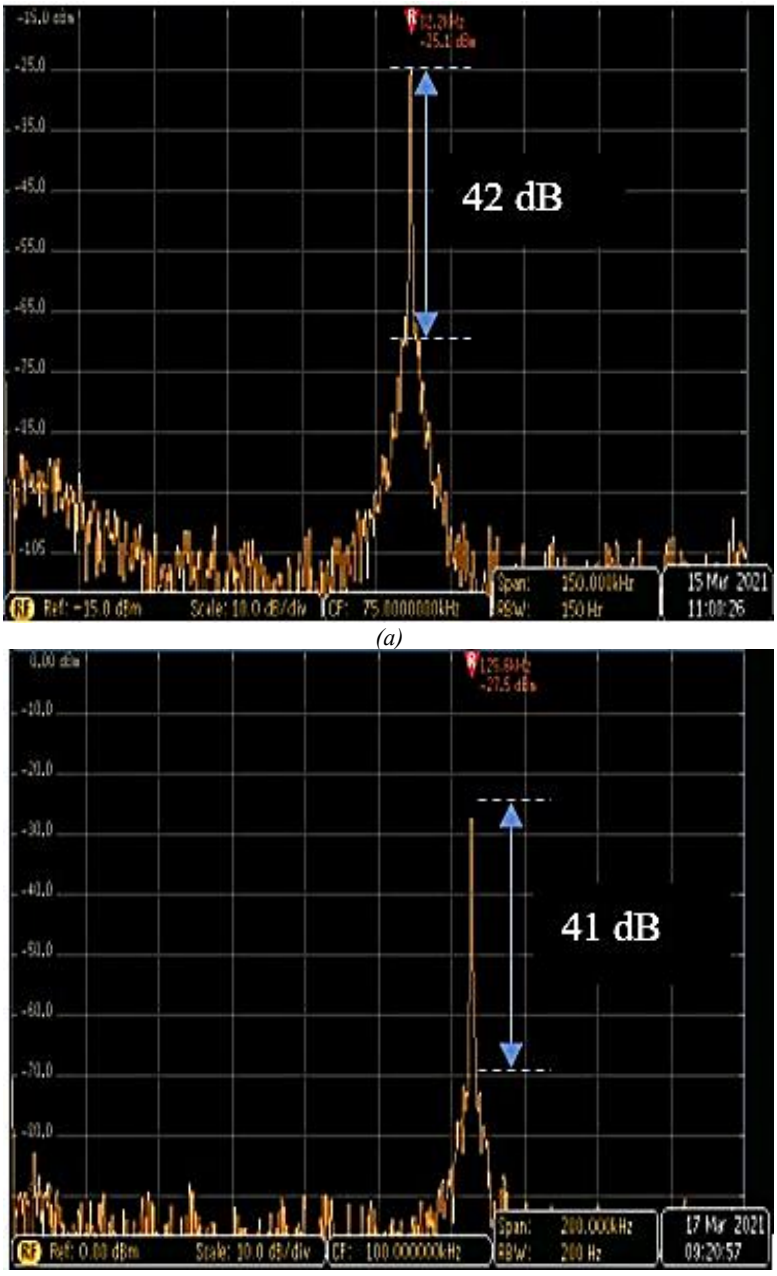

(a)

(b)

Fig. 14. SNR value of (a) 1:1 MWCNT-PVA (b) 2:3 MWCNT-PVA SA (colour online)

Some experiments have been conducted in passively Q-switched fiber laser using MWCNT SA and observed the output as below Table 2. However no experiment has been experimented with two different ratios of MWCNT in the same experimental setup.

Table 2. Output value of existing experiment using MWCNT SA

Author	Gain medium	Pump power (mW)	Repetition rate (KHz)	Operating Wavelength (nm)	Pulse width (μs)	Pulse energy (nJ)
Sity Nur Fatin [29]	EDF	103 - 215	76.92	1558.2	1.9	3.39
Azooz [29]	EDF	39 - 65.3	48.22	1534.5	5.3	99.75
	TDF	80.0 - 121.1	10.38	1846.4	17.52	11.34

Table 3 shows the overall performance, namely repetition rate, pulse width, pulse energy, output power and SNR. When MWCNT-PVA was used as SA in the same Q-switched fiber laser ring cavity, the highest pulse energy of 24.57 nJ with 1:1 MWCNT-PVA SA and output power of 2.84 mW with 2:3 MWCNT-PVA SA were recorded. In terms of repetition rate and pulse width, 2:3 MWCNT-PVA SA exhibited the best output performance of 130 kHz and

3.94 μs. The 1:1 MWCNT:PVA mix required a lesser pump power to produce Q-switched laser pulse train. With the reduction of MWCNT composition, the wavelength shifts from longer to shorter, due to the SA-induced insertion loss [28].

Table 3. Comparison of different ratio (1:1 and 2:3) of MWCNT-PVA SA

MWCNT: PVA	Pump Power (mW)	Operating Wavelength (nm)	Repetition Rate (kHz)	Pulse width (μs)	Pulse energy (nJ)	Output power (mW)	SNR Value (dB)
1:1	31.3 - 121.5	1557.98	89.13	4.43	24.57	2.19	42
2:3	83.6 – 177.6	1557.48	134.2	3.94	21.15	2.84	41

Several other strategies can be examined to enhance the outcomes, most notably: Optimize the concentration, thickness, and uniformity of the SA films, investigate heat dissipation methods for the SA to avoid degradation during long-term operation, use alternate gain fibers or heavily doped EDF to improve gain efficiency, use linear cavity to increase pulse stability.

4. Conclusion

Passive Q-switched all-fibre EDFL laser cavity with self-starting and stable pulsed laser output has been effectively demonstrated with MWCNT-PVA Sas fabricated in 1:1 and 2:3 ratios. The narrowest pulse widths were 4.43 μs and 3.94 μs, respectively, using 1:1 and 2:3 MWCNT-PVA SAs, that were generated at maximum repetition rates of 89.13 kHz and 134.2 kHz. The comparison between 2:3 Q-switched pulse lasers and 1:1 MWCNT-PVA revealed that the former achieved the maximum pulse energy and increased SNR value, while the latter produced greater instantaneous and average output power, repetition rate, and pulse width. These SAs have a wide range of potential applications in both commercial and future research and development, as observed from their SNR value and instantaneous power.

Acknowledgements

This research work is funded by the Universiti Teknologi Malaysia under UTM Fundamental Research (Q.K130000.3843.22H96).

References

[1] D. Li, J. Zhu, M, Jiang, D. Li, H. Wu, J. Han, Z. Sun, Z. Ren, Appl. Phys. B **125**, 11 (2019).
[2] M. M. Mafroos, N. Ameelia, H. H. Jameela, A. Hamzah, International Journal of Integrated Engineering **15**, 170 (2023).
[3] K. M. Musthafa, A. Hamzah, O. W. Ling, A. H. A. Rosol, N. Mohamed, M. M. Mafroos, S. Harun, Journal of Advanced Research in Applied Sciences and Engineering Technology **32**, 119 (2023).
[4] B. Dong, J. Hu, C. Yu, J. Hao, Opt. Commun. **285**, 3864 (2012).
[5] X. D. Wang, Opt. Commun. **346**, 21 (2015).
[6] D. Sun, X. Xu, J. Chen, W. Shi, L. Sun, S. Chu, S. Ruan, Opt. Laser Technol. **136**, 106781 (2021).
[7] M. M. Mafroos, H. H. J. Sapingi, A. B. Hamzah, Indonesian Journal of Electrical Engineering and Computer Science **28**, 227 (2022).
[8] J. Liu, J. Xu, P. Wang, Opt. Commun. **285**, 5319 (2012).
[9] M. F. A. Rahman, A. Dhar, S. Das, D. Dutta, M. C. Paul, M. F. M. Rusdi, A. A. Latiff, K. Dimyati, S. W. Harun, Optical Fiber Technology **43**, 67 (2018).
[10] W. Zhou, X. Fan, H. Xue, R. Xu, Y. Zhao, X. Xu, D. Tang, D. Shen, Opt. Express **25**, 1815 (2017).
[11] M. M. Najm, A. S. Al-Hiti, B. Nizamani, H. Arof, P. Zhang, M. Yasin, S. W. Harun, Optik **242**, 167073 (2021).
[12] P. Yu, S. E. Lowe, G. P. Simon, Y. L. Zhong, Materials Science and Engineering **20**(5-6), 329 (2015).
[13] G. A. Kumar, International Conference on Emerging Trends of Research in Applied Sciences & Computational Techniques, Jodhpur Institute of Engineering & Technology (JIET), Jodhpur, Rajasthan, India, 2014, p.109
[14] A. A. Shakaty, J. K. Hmood, B. R. Mahdi, R. I. Mahdi, A. A. Al-Azzawi, Opt. Laser Technol. **146**, 107569 (2022).
[15] K. Y. Lau, P. J. Ker, A. F. Abas, M. T. Alresheedi, M. A. Mahdi, Opt. Commun. **435,** 251 (2019).
[16] O. W. Ling, A. Hamzah, N. Mohamed, M. M. Mafroos, 4th International Conference on Smart Sensors and Application (ICSSA), 34 (2022).
[17] W. Qiao, Z. Xiaojun, L. Zongsen, W. Yonggang, S. Liqun, N. Hanben, Optics Express **22**, 14782 (2014).
[18] N. M. Radzi, A. A. Latif, M. F. Ismail, J. Y. C. Liew, E. Wang, H. K. Lee, N. Tamcheck, N. A. Awang, F. Ahmad, M. K. Halimah, H. Ahmad, Results in Physics **16**, 103123 (2020).
[19] Y. Zhou, K. Zhang, T. Wang, W. Bi, M. Liao, G. Zhao, Y. O. Fang, Results in Optics **9**,100302 (2022).
[20] S. A. Sadeq, S. K. Al-Hayali, S. W. Harun, A. Al- Janabi, Results in Physics **10**, 264 (2018).
[21] J. Koo, J. Lee, J. Kim, J. H. Lee, Journal of

Luminescence **195**, 181 (2018).
[22] Cuihong Jin, Shaoxuan Jiang, Chen Xu, Delong Yang, Peng Yang, Chenning Tao, Si Luo, Qiang Ling, Yusheng Zhang, Yating Zhou, Opt. Commun. **549**, 129908 (2023).
[23] J. S. S. Neto, D. K. K. Cavalcanti, L. E. da Cunha Ferro, H. F. M. de Queiroz, R. A. A. Aguiar, M. D. Banea, Journal of Carbon Research **9**, 4, (2023).
[24] M. A. Ismail, S. W. Harun, H. Ahmad, M. C. Paul, Fiber Laser, IntechOpen, London (2016).
[25] K. M. Musthafa, A. Hamzah, F. Al Ghifarry, O. W. Ling, H. A. Rosol, Journal of Advanced Research in Applied Sciences and Engineering Technology **41**, 18 (2024).
[26] N. Alina Afifi Norizan, M. Quisar Lokman, S. Nur Fatin Zuikafly, H. Yahaya, F. Ahmad, S. Wadi, Journal of Telecommunication, Electronic and Computer Engineering **10**(2-7), 27 (2018).
[27] Y. I. Hammadi, T. S. Mansour, International Journal of Engineering and Technology **07**, 298 (2018).
[28] S. N. F. Zuikafly, F. Ahmad, M. H. Ibrahim, S. W. Harun, EPJ Web of Conferences **162**, 01014 (2017).
[29] S. M. Azooz, M. H. M. Ahmed, F. Ahmad, B. A. Hamida, S. Khan, H. Ahmad, S. W. Harun, Science Direct **126**(21), 2950 (2015).

*Corresponding author: azurahamzah@utm.my